J Nanostruct 9(4): 712-722, Autumn 2019

RESEARCH PAPER

Catalyzed Schiff Base Synthesis over Bifunctionalized Cobalt/Zinc-Incorporated Mesoporous Silica Nanoparticles under UV Irradiation

Homa Choopan Tayefe[1], Mohammad Reza Sazegar[1], Ali Mahmoudi*[1], Khosrow Jadidi[2]*

[1]*Faculty of Chemistry, Islamic Azad University, North Tehran Branch, Tehran, Iran*
[2]*Faculty of Chemistry, Shahid Beheshti University, Tehran, Iran*

ARTICLE INFO

Article History:
Received 04 July 2019
Accepted 28 August 2019
Published 01 October 2019

Keywords:
Cyclohexanone 2,4-Dinitrophenylhydrazone
CZ-MSN
Mesoporous Silica
Schiff Base
UV Irradiation

ABSTRACT

A novel series of the cobalt/zinc-mesoporus silica nanoparticles (denoted by CZ-MSN) catalysts with Si/Zn molar ratio of 10 and 1, 3, 5 and 7 wt% cobalt were synthesized using post-synthesis methods. The samples were characterized by XRD, SEM, FTIR, TEM and nitrogen adsorption-desorption methods. An increasing amount of cobalt species from 1 to 7 wt% at constant ratio of Si/Zn, leading the reduction of catalyst surface from 408 m^2g^{-1} to 322 m^2g^{-1}. The catalytic activities for the synthesis of the Schiff base was investigated through the reaction of cyclohexanone with 2,4-dinitrophenylhydrazine under UV irradiation. The activity of the catalysts in the formation of the Schiff base followed the cobalt amounts of 0<1<7<3<5. The sample with cobalt 5 wt% exhibited the highest performance with the conversion and selectivity of 98 and 97% respectively, under UV light at 298 K for 10 min. The superior catalytic performance of the catalyst with cobalt 5 wt% includes high yield, low reaction temperature, short reaction time and eco-friendly. We assume that the reason would be related to the stronger metal-support interaction and metals dispersion. This study provides the new perspective on the synthesis of CZ-MSN towards an excellent performance of Schiff base structure under UV irradiation.

How to cite this article
Choopan Tayefe H, Sazegar M, Mahmoudi A, Jadidi K. Catalyzed Schiff Base Synthesis over Bifunctionalized Cobalt/Zinc-Incorporated Mesoporous Silica Nanoparticles under UV Irradiation. J Nanostruct, 2019; 9(4): 712-722.
DOI: 10.22052/JNS.2019.04.013

INTRODUCTION

Synthesis of chemical compounds is often carried out by using the commercial homogeneous catalysts. Although homogeneous catalysts provide faster reaction rates in comparison with the heterogeneous catalysts, the catalysts separation from the reaction mixture and work-up the products are more difficult [1]. In addition, the generation of undesirable products as by-products, low yield and formation of toxic residues are the other drawbacks of this type of chemical synthesis [2]. Recently, replacement of homogeneous catalysts by heterogeneous solid catalysts have been noticed by the researcher in order to reduce the mentioned problems. Since the suitable solid catalysts should be recovered after the reaction and recycled several times, therefore they are economic and friendly environmental materials [3,4]. In recent years, ordered mesoporous silica materials such as MCM-41 and SBA-15 with high surface areas, large pore sizes and pore volumes and also well-defined hexagonal structures have been employed as the heterogeneous solid supports [5,6]. These nanomaterials showed good flexibility, high thermal and mechanical stability to modify with various functional groups and metals onto the surface. These mesoporous silica nanomaterials possesses ordered porous network

* *Corresponding Author Email: m_r_sazegar@yahoo.com, mahmoudiali.ac@gmail.com*

for unique diffusion of substrates and reaction products. These properties have attracted interest for their application as the catalyst-immobilization matrices [7,8].

EXPERIMENTAL

Materials

Tetraethylorthosilicate (denoted by TEOS, purity 99%) as the silicon source, cetyltrimethylammonium bromide (denoted by CTAB, purity 98%) as a template, ammonia solution (28%) and ethanol (96%) in the present study were purchased from Merck Company. Also zinc acetate dihydrate for analysis (99.5%) and cobalt acetate tetrahydrate for analysis (99%) were prepared from Merck Company.

Preparation of transition-metal (Co, Zn) incorporated MSN

Mesoporous silica nanoparticles (denoted by MSN) was synthesized by the sol-gel method in the basic conditions [9]. Typically, Cetyltrimethylammonium bromide (CTAB, 1.17 g) was dissolved in a solution of double distilled water (215 g) and ethyl alcohol (35 mL), and then an aqueous ammonia solution (8.5 mL, 28%) was added. After vigorous stirring for approximately 25 min at 298 K, tetraethylorthosilicate (TEOS, 1.8 mL) was added to the mixture. The mixture was stirred for an additional 120 min at 298 K and allowed to rest for 24 h at the same temperature. The gel composition used in the synthesis of the pure MSN was 1 TEOS : 0.6 CTAB : 14 NH_3 : 87 ethanol : 1046 H_2O. The sample was collected by centrifugation at 20,000 rpm for 20 min and washed with deionized water and absolute ethanol three times and dried at 383 K for 8 h prior to calcination. The surfactant was removed by calcination of MSN (1 g) in air at 823 K for 3 h.

Zn-grafted MSN (denoted as Zn-MSN-10) was prepared by incorporation of zinc into the pure MSN. Zinc acetate dihydrate was used as a precursor of zinc. The initial molar ratios of Si/Zn was 10. The Zn-MSN samples were synthesized by adding MSN (1 g) into an aqueous solution (50 mL) of zinc acetate (0.11 g) at 353 K for 12 h followed by centrifugation and drying at 383 K overnight prior to calcination in air at 823 K for 4 h with a heating rate of 1 K min^{-1}. The CZ-X-MSN catalysts were prepared by impregnation of Zn-MSN (1 g) with 1, 3, 5 and 7 wt% cobalt solution followed by calcination in air at 823 K for 3 h. Cobalt acetate tetrahydrate was applied as a source of cobalt. The synthesized samples named CZ-1-MSN, CZ-3-MSN, CZ-5-MSN and CZ-7-MSN which 1, 3, 5 and 7 were the cobalt percentages. General name of these catalysts is CZ-X-MSN.

Catalytic performance

The catalytic activity of the CZ-X-MSN catalyst was investigated for the Schiff base formation via the condensation reaction. The details of this study are explained in the following section.

Typical experimental protocol

A solution of 2,4-dinitrophenylhydrazine (denoted by 2,4-DNPH, 0.02 mol) in ethanol (20 mL) was prepared. Then respectively CZ-X-MSN (0.01 wt%) and cyclohexanone (0.02 mol) was slowly added into the 2,4-DNPH solution at the room temperature and stirred at 298 K under UV light for 10 min. The samples were taken at regular intervals and the concentrations of cyclohexanone, 2,4-DNPH and Schiff base were identified by GC-Mass spectrometry (detector HP 5971) and analyzed using chrompak CP 9000 GC equipped with an RTX-50 capillary column and a flame ionization detector. The dodecane was chosen for the internal standard.

The conversion of cyclohexanone to cyclohexanone 2,4-dinitrophenylhydrazone (denoted by CHDN) (X_{CHDN}%), the yield (Y_{CHDN}%) and selectivity (S_{CHDN}%) of this Schiff base production were calculated according to eq (1)–(3), respectively:

$$X_{CHDN}\,(\%) = \frac{C_i - C_f}{C_f} \times 100 \quad (1)$$

$$Y_{CHDN}\,(\%) = \frac{n_y}{n_c} \times 100 \quad (2)$$

$$S_{CHDN}\,(\%) = \frac{n_y}{n_i - n_f} \times 100 \quad (3)$$

Where C_i and C_f are the concentrations of cyclohexanone at the initial and final reaction times, respectively; n_y and n_c are the number of moles of the yielded and calculated CHDN, respectively; and n_i and n_f are the number of moles of cyclohexanone at the initial and final reaction times, respectively.

Reusability testing

The reusability of CZ-X-MSN for the CHDN

production (%) at 298 K under UV irradiation was studied after it was used six times [10]. The catalyst was washed with dichloromethane (2×10 mL) and dried under vacuum at 358 K for 4 h. The weight of the catalyst, its catalytic activity and the product were measured after each reaction. After each reaction, the catalyst was subjected to FTIR and XRD to study its properties.

Characterization of the CZ-X-MSN catalysts

The crystallinity of catalysts was measured with a Bruker Advance D8 X-ray powder diffractometer with Cu Ka (l = 1.5418 Å) radiation as the diffracted monochromatic beam at 40 kV and 40 mA. Nitrogen adsorption-desorption analysis was conducted on a Quantachrome Autosorb-1 at 77 K. Before the measurement, the sample was evacuated at 573 K for 3 h. The bulk Si/Zn ratio of the Zn-MSN-10 was determined by Bruker S4 Explorer X-ray fluorescence spectroscopy (XRF) using Rh as anode target material operated at 20 mA and 50 kV. Fourier transform infrared (FTIR) measurements were carried out using an Agilent Carry 640 FTIR spectrometer.

The morphology and average particle size of the catalyst were estimated from transmission electron microscopy (TEM) images using a JEOL JEM-2100 transmission electron microscope. Prior to the TEM measurements, the powder samples were ground and subjected to ultrasonic treatment in hexane for 10 min. A drop of the suspension was dried on a copper TEM sample grid. A scanning electron microscope equipped with an energy dispersion X-ray spectrometer (EDX) was conducted on SEM (JEOL JSM-6701 F) to observe the morphology as well as to obtain the elemental analysis of the catalyst using. Before observation by SEM-EDX, the sample was coated by Pt using a sputtering instrument. The organic compounds were characterized by ^{1}H and ^{13}C NMR spectra recorded on Bruker DRX–500 AVANCE spectrometer in DMSO at ambient temperature.

RESULTS AND DISCUSSION

Catalyst characterization

The CZ-X-MSN catalysts were synthesized using the post-synthesis technique via the grafting zinc and cobalt into the parent MSN. The XRD patterns of MSN, Zn-MSN-10 and CZ-X-MSN samples with constant Si/Zn molar ratio of 10 in the low and high angle degrees are given in Fig. 1., which X is equal to 1, 3, 5 and 7 wt% of cobalt atom

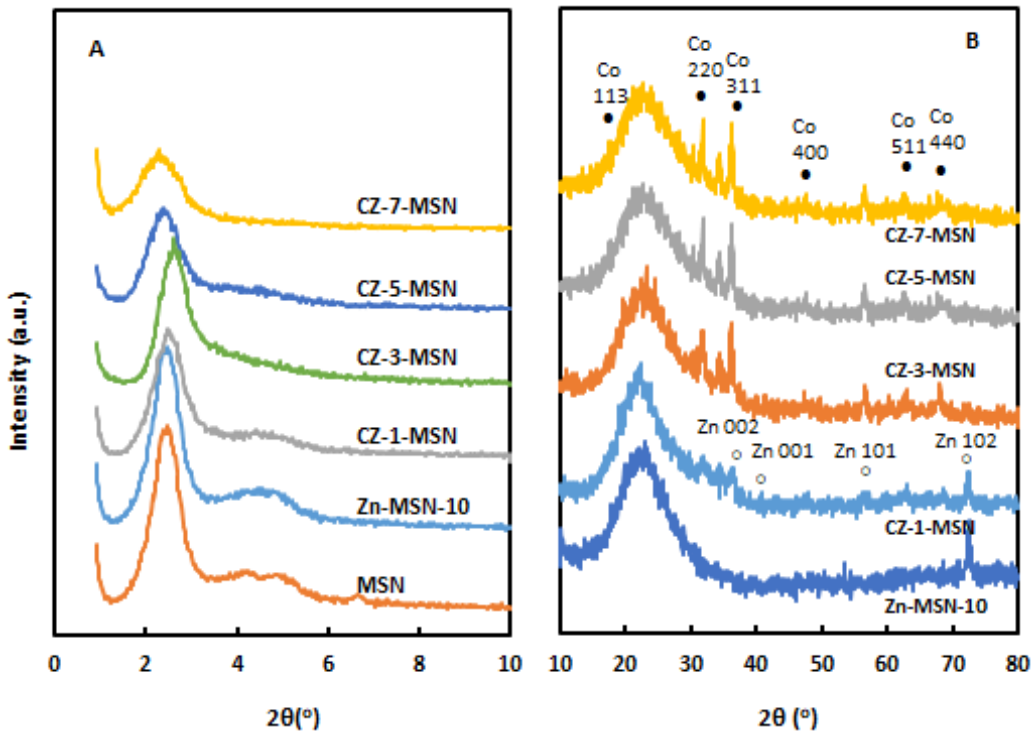

Fig. 1. XRD patterns: (A) low degree at 0-10° for MSN, Zn-MSN-10 and CZ -1-10 to CZ-7-MSN, (B) high degree at 10-80° for Zn-MSN-10 and CZ-1-MSN to CZ-7-MSN.

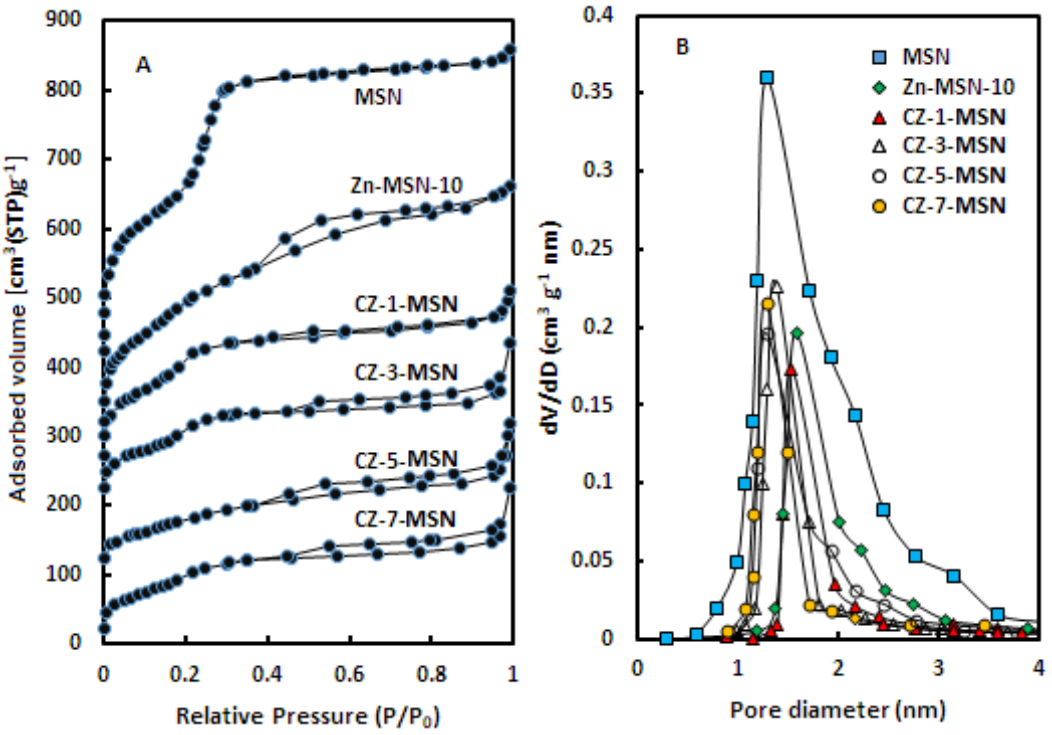

Fig. 2. (A) Nitrogen adsorption-desorption isotherms, (B) pore size distribution for MSN, Zn-MSN-10 and CZ-X-MSN.

respectively. In Fig. 1A, three peaks at a low angle degree were observed for the pure MSN which included the intense diffraction peaks of 100 between 2θ = 1.75–2.75° and two small diffraction peaks of 110 and 200 at about 2θ = 4–6°. These peaks indicated the presence of two-dimension hexagonal (*p6*mm) structure with a d_{100}-spacing of approximately 3.65 nm. Incorporation of zinc and cobalt atoms into the MSN decreased the intensity of the peak to 100 which evidenced to the less order mesoporous structures [5]. Moreover, the shift of the peak position from 1.75° to 2.75° might be arising from the substitution of Si with zinc and cobalt atoms which led to the formation of Zn-O-Si and Co-O-Si structures. Fig. 1B shows the high angle XRD patterns at 10-90° for the MSN, Zn-MSN-10 and CZ-X-MSN samples. X-ray microanalysis of these catalysts revealed the presence of zinc and cobalt elements in their structures with different cobalt amounts in the constant Si/Zn molar ratio. The observed peaks of 113, 220, 311, 511 and 440 planes for the CZ-X-MSN catalysts at the high degree characteristic of a Co_3O_4 phase indicating the formation of the amounts of cobalt oxide microcrystallites on the walls/surface of the nanomaterials [11, 12]. The peaks corresponded to diffractions of 001, 002, 101 and 102 planes exhibited the existence of zinc oxide phase in these nanostructures [13].

In conclusion, the XRD patterns revealed that the structure of the CZ-X-MSN catalysts go toward amorphous structures by increasing the amount of X and only cobalt oxide is formed as a crystalline structure on the catalyst surfaces. The presence of the large cobalt and zinc species into the MSN structure resulted in an increase in the layer spacing. Substitution of Zn and Co species into the MSN framework were also reflected by the presence of the peaks with higher intensity for the CZ-X-MSN catalysts, as shown in the diffraction patterns of Fig. 1B. The results showed that with

Table 1 Physical characteristics of the MSN, Zn-MSN-10 and CZ-X-MSN samples

Sample	d_{100} (nm)	a_0 (nm)	S (m^2/g)	Vp (cm^3/g)	W (nm)
MSN	3.60	4.16	887	0.71	3.42
Zn-MSN-10	3.89	4.45	465	0.40	3.37
CZ-1-MSN	3.82	4.41	408	0.36	3.50
CZ-3-MSN	3.43	4.00	301	0.3٥	4.34
CZ-5-MSN	3.63	4.20	330	0.3٤	4.31
CZ-7-MSN	3.66	4.23	322	0.3٢	4.20

d_{100}, *d*-value 100 reflections; a_0, pore center distance is equal to d_{100}*2/√3; *S*, BET surface area (m^2/g) obtained from N_2 adsorption-desorption; V_p, total pore volume (mL/g); *W*, pore size (nm) obtained from BJH method.

metal loading into the MSN structure the *d*-spacing slightly increased (Table 1).

Though the initial amount of Si/Zn molar ratio of 10 was calculated for Zn-MSN, the XRF analysis showed that this ratio into the framework was 9.3. In addition, the results of XRF analysis showed that the Si/Zn ratios of the Co/Zn-MSN frameworks was 9.3 and the amount of cobalt were 1, 3, 5 and 7 wt% for CZ-1-MSN, CZ-3-MSN, CZ-5-MSN, and CZ-7-MSN, respectively. Furthermore, intercalation of cobalt and zinc cations within the interlayer spacing of MSN resulted in an increase in the basal spacing due to the substitution of exchangeable interlayer atoms. Substitution of Zn and Co atoms instead of Si atoms into the framework was also reflected by the presence of peaks with higher intensities for the CZ-X-MSN catalysts, as shown in the diffraction patterns of Fig. 2B. The higher angle XRD pattern shows the presence of weak peaks characteristic of a Co_3O_4 phase indicating the formation of small amounts of cobalt oxide microcrystallites on the walls of the metallosilicate. The diffractogram of the CZ-X-MSN catalysts shows more peaks of the Co_3O_4 phase, whereas the matrix is amorphous [14]. Table 1 shows the physical properties of the MSN, Zn-MSN-10, CZ-1-MSN, CZ-3-MSN, CZ-5-MSN, and CZ-7-MSN catalysts.

The surface area was decreased from 887 m^2g^{-1} for MSN to 322 m^2g^{-1} for CZ-7-MSN which indicated to the loading of Zn and Co metals onto the catalyst surfaces. These results indicated a direct relationship between metal content and activity of the catalysts which led to change in the pore diameter of the catalysts which was probably due to the presence of extra-framework structure (EFS) inside the pores [10]. The grafting Zn-MSN-10 with cobalt species in different percentages of 1, 3, 5 and 7 were plugged the pores of Zn-MSN-10 with a size of around 3.35 – 4.25 nm. The number of the pores plugged was increased with the amount of zinc and cobalt into the structure which led to the decrease in the pore volume from 0.71 cm^3g^{-1} for MSN to 0.34 cm^3g^{-1} for CZ-7-MSN (Table 1). The Zn and Co species were placed inside and/or on the mouth of the pores [9].

The presence of two metals with positive oxidation number causes a repulsion between these cations which led to enhance in the pore diameters from 3.50 nm to 4.20 nm for CZ-1-MSN and CZ-7-MSN respectively. Fig. 2 shows the nitrogen adsorption-desorption isotherms and the pore size distribution of MSN, Zn-MSN-10, CZ-X-MSN catalysts which was calculated by the NLDFT method. The nitrogen adsorption-desorption isotherm patterns of the pure MSN sample showed type IV isotherms which are attributed to the ordered mesoporous silica nanoparticles with cylindrical pores (Fig. 2A). The isotherm of these nanomaterials has shown the inflection characteristic of capillary condensation at a relative pressure (P/P_0) of around 0.1-0.3 which was evidenced to the presence of the porous structures with the small and uniform mesopore structures [15].

An observed increase at the high relative pressure (P/P_0) of around 0.9–1.0 in the CZ-X-MSN catalysts is evidenced to the presence of the external-framework porosity especially for the samples with X=3, 5 and 7. These isotherms were indicated to the existence of less ordered mesoporous structure due to the incorporating these transition metals into the MSN. An increase in the cobalt atoms has altered the catalyst properties. The surface area and the pore volume were decreased due to the pore plugging by these transition metals. Some walls dissolved by desilication phenomenon because of the metal grafting which new mesopore systems with slit-like pores were formed. The appearance of H2 type hysteresis loops is a strong evidence for this statement (Fig. 2B).

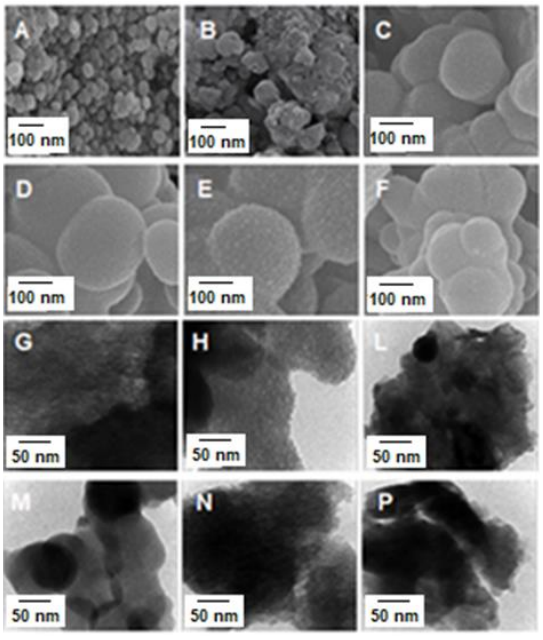

Fig. 3. (A-F) SEM images and (G-P) TEM images of MSN, Zn-MSN-10, CZ-1-MSN, CZ-3-MSN, CZ-5-MSN and CZ-7-MSN, respectively.

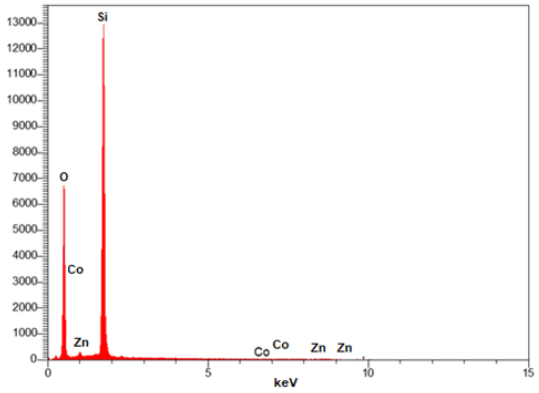

Fig. 4. Energy-dispersive X-ray spectroscopy of the CZ-X-MSN sample.

The morphology of MSN, Zn-MSN-10, CZ-1-MSN, CZ-3-MSN, CZ-5-MSN and CZ-7-MSN were studied using SEM and TEM images. The SEM images of these samples were shown in Fig. 3(A-F) which indicated to uniform spherical particles with particle size of 70–150 nm. The 2D mesoporous structures were confirmed by TEM analysis (Fig. 3G–P). The TEM images confirmed the ordered structures of these nanomaterials with the metals dispersion [16]. The obtained results are in agreement with the results from the low-angle XRD patterns and nitrogen physisorption analysis.

As a typical sample, the EDX result of CZ-1-MSN was shown in Fig. 4 which indicated the presence of silicon, zinc, cobalt and oxygen in the CZ-X-MSN materials. No other peaks related to any impurity were detected in the EDX analysis. Fig. 5 has shown the FTIR spectroscopy of the MSN, Zn-MSN-10 and CZ-X-MSN samples at the region of 400-4000 cm^{-1}. The sharp band at about 3435 cm^{-1} is assigned to the hydration state of silica which located on the external surface of the mesoporous structure [17]. Loading zinc and cobalt decreased the H-bonds of the hydroxyl groups on the MSN due to the reaction of silanol group with the metals which formed the sharper peaks at this range of wavenumber. The results show that all peaks of the CZ-X-MSN catalysts are sharper than the MSN and Zn-MSN-10 samples. This change in the shape of peaks may be due to the formation of the metalosilicate framework and the interaction of metals with the Si atom through the O atom (Si-O-M) [9].

It was not observed any noticeable differences in the band intensities in the region of 3435 cm^{-1} for the pure and modified MSN samples, which indicates that they have a comparable primary particle size and have not any significant differences in the d_{100}-spacing or pore diameters [18]. Three vibration peaks of FTIR spectrum located at the regions of 1078 and 467 cm^{-1} are associated with the Si-O stretching frequency in the mesoporous silica materials, whose peaks at 467 and 1078 cm^{-1} correspond to bond O–Si–O and bond Si–O–Si, respectively. While the absorption peak at the region of 795 cm^{-1} indicated the Si-O-Si bending vibration in the catalysts structures [19]. The activity of the pure MSN, zinc and cobalt-modified MSN catalysts was investigated in Schiff base reaction. In a condensation reaction, cyclohexanone as a ketone was reacted with 2,4-dinitrophenylhydrazine under UV light which resulted in a Schiff base of CHDN.

Fig. 6 shows the conversion of 2,4-DNPH to CHDN using different catalysts of MSN, Zn-MSN-10 and CZ-X-MSN under UV conditions. Condensation reactions were compared using a blank and conventional homogenous catalyst,

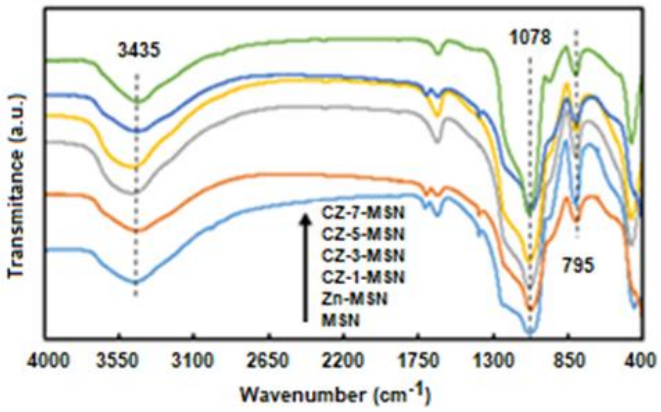

Fig. 5. FTIR spectra of MSN, Zn-MSN-10 and CZ-X-MSN at the region of 400-4000 cm^{-1}.

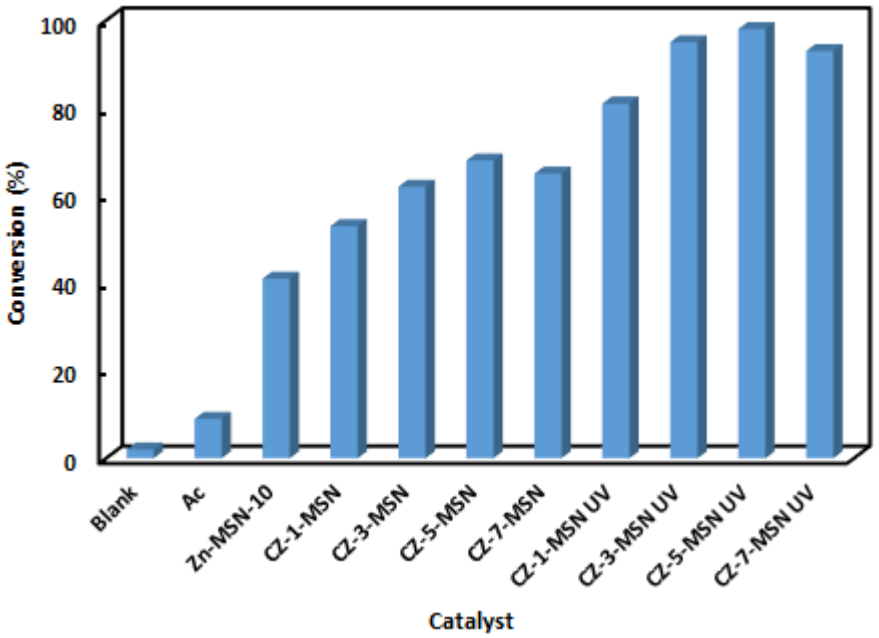

Fig. 6. Conversion of cyclohexanone to CHDN with the blank, acetic acid, Zn-MSN-10 and CZ-X-MSN samples with X=1,3,5 and 7 without and with UV irradiation

such as acetic acid, when heterogeneous metal-grafted MSNs were used. The results showed that the blank sample and acetic acid exhibited 2 and 9% conversion, respectively, at 298 K for 30 min. While, the Zn-MSN-10, CZ-1-MSN, CZ-3-MSN, CZ-5-MSN and CZ-7-MSN samples were showed the conversion of 41, 53, 62, 68 and 65%, respectively, at 298 K for 30 min. While, the conversion of cyclohexanone to CHDN over the CZ-X-MSN catalysts showed 81, 95, 98 and 93% under UV irradiation at 298 K for 10 min.

The highest conversion of 98% probably was related to the strongest metal-support interaction and more suitable transition metal dispersion, which led to the highest catalytic performance. The results exhibited that the synthesis of CHDN over CZ-X-MSN revealed an increase the cyclohexanone conversion from 1 to 5 wt% of cobalt and a decrease conversion for the sample with 7 wt% cobalt may be due to the presence of the inactive cobalt species into the crystal structure [20].

In the Schiff base synthesis, the turnover frequency (TOF) is the number of moles of cyclohexanone that a mole of the CZ-X-MSN catalyst can produce per unit time, before becoming inactive. Therefore, TOF was determined from the rate of CHDN synthesis per time (min). The TOF of CHDN synthesis over CZ-X-MSN is shown in Fig. 7. However, the TOF increased with the reaction time and the sample of CZ-5-MSN showed the highest conversion of cyclohexanone to CHDN product after 10 min under UV irradiation.

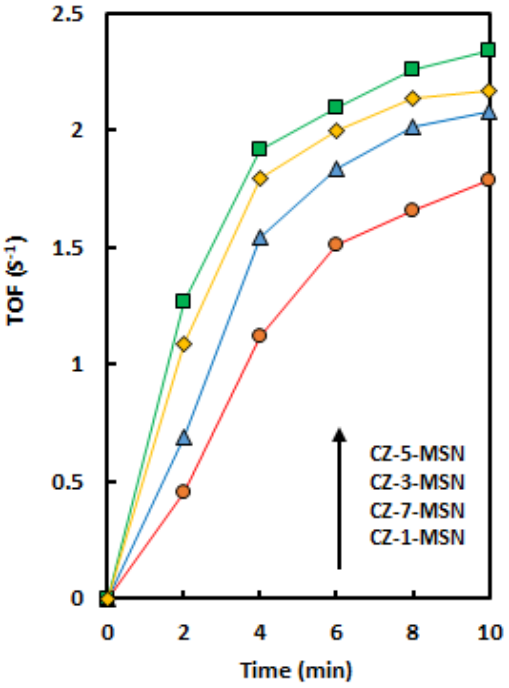

Fig. 7. Turnover frequency of CHDN production during the Schiff base synthesis over the CZ-X-MSN catalysts under UV irradiation at 298 K for 10 min.

Heterogeneous solid catalysts are capable to catalyze the several organic reactions including double bond formation such as Schiff base (imine), Azo and carbonyl groups, Michael addition, Claizen-Schmidt reaction, Knovenagel condensation, transesterification, hydrogenation, amination, alkylation and etc. [4,9]. Many biologically active compounds with the medicinal properties such as amino acids and organic compound drugs possess Schiff base (Imine) structure, an azomethine group (-HC=N-), show antimicrobial, anticancer, antifungal, and anti-inflammatory activity [22]. This structure is formed through the condensation reaction of a ketone/aldehyde with a primary amine (Fig. 8) which is normally obtained under acid or base conditions [23]. So far, some Schiff base complexes (organometallic compounds) are used as the excellent catalysts for the various chemical reactions at the high temperatures and in the presence of moisture. The Schiff base group is used for DNA binding and cleavage properties under physiological conditions, to act as a diagnostic agent in the medicinal applications and also for genomic research [24].

Phenylhydrazine and its dinitro derivatives (Brady's reagent) are the chemical reagents which are used to recognize the presence of the carbonyl group into the structure. This reaction is commonly catalyzed by homogeneous acids or bases in a liquid phase and lastly, Phenylhydrazone or Dinitrophenylhydrazone (denoted by DNPH) are produced. The substitution of liquid acid/base by the solid catalysts is a serious challenge in the synthesis of these organic compounds. The new environmental legislature drives to replace solid catalysts instead of liquid media which leads to reducing pollution and waste reduction [25].

In the present work, we introduced a novel series of the bifunctional mesoporous silica nanoparticles (denoted by BMSN) with different cobalt and zinc loading on to the mesoporous silica nanoparticles (denoted by CZ-X-MSN) surface and investigated their catalytic activities for the synthesis of cyclohexanone 2,4-dinitrophenylhydrazone (denoted by CHDN) under UV irradiation at room temperature for 10 min. The effects of transition-metals (Co and Zn) grafted into MSN on the Schiff base formation were explained in detail. The synthesis of CHDN was carried out through the reaction between cyclohexanone and 2,4-dinitrophenylhydrazine (denoted by 2,4-DNPH) over these catalysts under UV conditions (Fig. 9).

Fig. 10 shows a proposed mechanism for the formation of a Schiff base system over the CZ-X-MSN catalysts at room temperature under UV light. 2,4-DNPH and cyclohexanone took part in a condensation reaction through the bond formation between carbonyl group of cyclohexanone and zinc atom into the catalyst framework and also a hydrogen bond formation between the oxygen atom of the catalyst and amine group of 2,4-DNPH component. The presence of UV light generates the radical species which make higher bond formation and lead to higher stability which resulting in higher conversion during the condensation reactions.

REUSE OF THE CZ-5-MSN CATALYST

Fig. 11 shows the reusable property of CZ-5-MSN for the synthesis of CHDN. After each condensation reaction, the catalyst was recycled

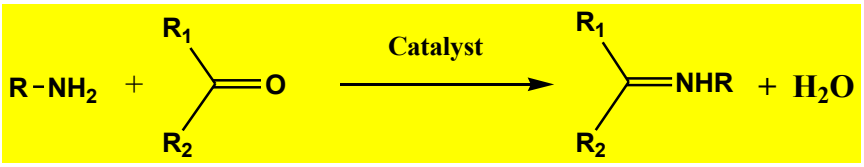

Fig. 8. Condensation reaction for Schiff base synthesis

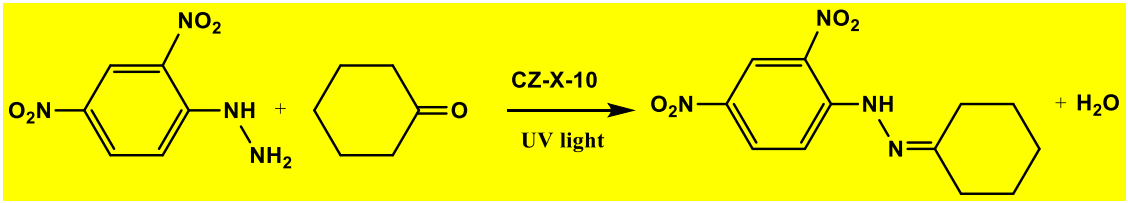

Fig. 9. Condensation reaction of cyclohexanone with 2,4-DNPH under UV light

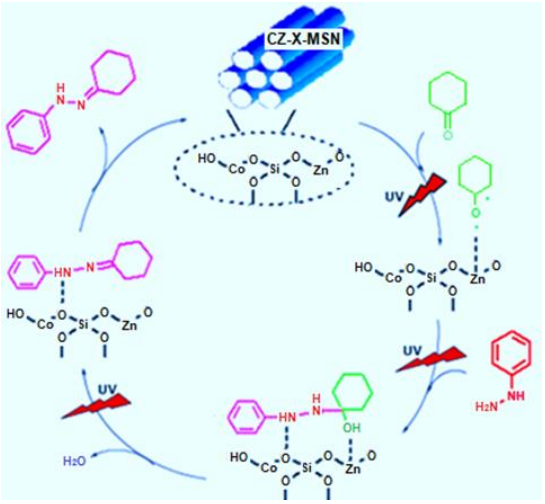

Fig. 10. Proposed mechanism of the CHDN synthesis over the CZ-X-MSN catalysts under UV irradiation

by washing with dichloromethane (2×10 mL) and drying under vacuum at 358 K for 4 h [21]. The catalyst was reused seven times without an essential loss in the catalyst weight and catalytic activity during each recycling process. The results showed a high stability in the catalyst structure through the lack of a serious decrease in the synthesis of CHDN. The yield was observed from 98% for the first reaction to 94% for the 8th condensation reaction which indicates the good reusability of the CZ-5-MSN catalyst. The FTIR spectra and XRD patterns (not shown) of CZ-5-MSN (as a symbol of the CZ-X-MSN samples) before and after Schiff base formation was an evidence to the high stability of this catalyst.

Table 2 shows the comparison of the Schiff base formation between CZ-X-MSN and various types of heterogeneous catalysts [26–29]. The results showed the high activity of the CZ-X-MSN samples (unless CZ-7-MSN), in comparison with the other catalysts such as mesoporous carbon, pure SBA-15 and MCM-41, PC-SBA-15, SBA-15-Co, MCM-41-NH_2, Al, Fe and Zn-MCM-41 and Zn-MSN-10. The sample of CZ-7-MSN exhibits a lower conversion and yield among of all CZ-X-MSN catalysts probably due to the presence of inactive cobalt atoms in its structure [20]. Mesoporous

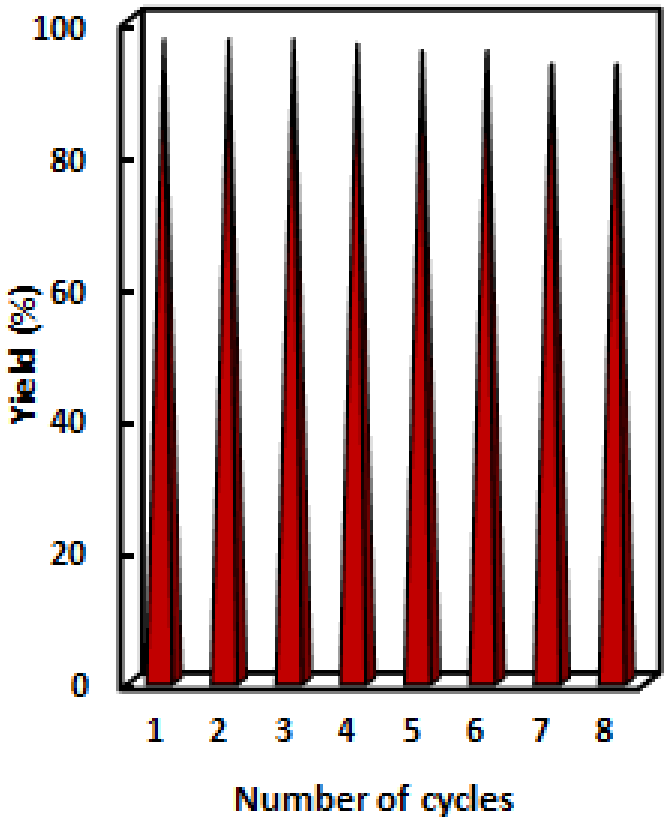

Fig. 11. Stability of CZ-5-MSN in the condensation reaction under UV irradiation at 298 K, after it was reused five times.

Table 2 The comparison of the Schiff base synthesis using the heterogeneous catalysts

Catalyst	Conversion (%)	Selectivity (%)	Yield (%)	Time (Min)	Temperature (K)	Ref.
CZ-1-MSN UV	81	95	76	10	298	This study
CZ-3-MSN UV	95	98.7	94	10	298	This study
CZ-5-MSN UV	98	98.5	97	10	298	This study
CZ-7-MSN UV	93	97.8	91	10	298	This study
Zn-MSN-10 UV	41	95	39	10	298	This study
Mesoporous carbon(PC)	20.6	97.1	20	300	373	20
Pc-SBA-15-8	77.3	96.5	74	300	373	20
Al-MCM-41	-	-	59	20	298	26
SBA-15	-	-	15.2	720	423	27
SBA-15-Co	-	-	16	720	423	27
MCM-41	-	-	85	60	298	28
MCM-41-NH_2	-	-	92	20	298	28
Fe_3O_4-MCM-41	-	-	95	40	298	28

structured-bifunctional catalysts of CZ-X-MSN (X=1,3 and 5) exhibited the high conversions, selectivity and yields in comparison with the other samples possess mono-functional structures possibly due to the uniform/suitable transition metals dispersion which led the formation of two different active sites on the MSN framework. Consequently, enough spaces were formed for the reaction of the reactants with more active sites inside and outside the catalysts structures. In addition, the significant advantages of using these catalysts were short time reaction, low reaction temperature, friendly environment and catalysts compatible in organic and aqueous media.

Following the mentioned procedure of the synthesis of CHDN over CZ-5-MSN was obtained as a crystalline powder in 97% yield; M.P. 159-160 °C.

^{1}H NMR (DMSO-d_6, 500 MHz, δ, ppm): 10.96 (1H, s), 8.83 (1H, s), 8.32-8.34 (1H, d), 7.82 (1H, d), 1.59-1.71 (4H, d), 2.40 (4H, t), 2.47 (2H, t). ^{13}C NMR (DMSO-d_6, 500 MHz, δ, ppm): 25.28, 25.86, 26.99, 27.42, 35.37, 116.24, 123.42, 129.20, 130.39, 136.92, 145.19, 163.30.

CONCLUSION

A novel series of the cobalt/zinc-MSN catalysts with Si/Zn=10 and 1, 3, 5 and 7 wt% cobalt as solid catalysts were synthesized using post-synthesis methods. X-ray diffraction and N_2 adsorption-desorption results confirmed the mesoporous structures with pore diameters range of 3.42 – 4.20 nm, and surface areas range of 408 m^2g^{-1} to 322 m^2g^{-1} for CZ-1-MSN and CZ-7-MSN respectively. The characterization results exhibited that the introduction of zinc and cobalt into the MSN influenced the properties of the catalysts which indicated the homogeneous metal dispersion.

These catalysts catalyzed Schiff base synthesis of CHDN followed the order of Zn-MSN-10<CZ-1-MSN<CZ-7-MSN<CZ-3-MSN<CZ-5-MSN, in which the cyclohexanone conversion to CHDN over CZ-5-MSN under UV light was 98% at 298 K for 10 min. The outstanding advantages of using CZ-5-MSN is including high yield, selectivity, low reaction temperature, quick work up and short reaction time. We assume that these advantages might be arising from large Co and Zn atoms, stronger metal-support interaction and more homogeneous metal dispersion. These properties promoted the catalytic performance for the Schiff base synthesis. The formation of CHDN over CZ-5-MSN was reused five times indicated to the high catalytic stability. The result of Schiff base synthesis showed that the zinc and cobalt grafted MSN with the molar ratio of Si/Zn=10 and cobalt atoms with 1, 3 and 5 wt% are able to catalyze the condensation reactions under UV conditions with high efficiency, low reaction time, low reaction temperature, energy consumption and environmental friendliness.

ACKNOWLEDGMENT

We express our appreciation to the late Prof. Sugeng Triwahyono, whose contribution to all our works were of great significance. We also thank from Islamic Azad University, North Tehran Branch for helping in this study.

CONFLICT OF INTEREST

The authors declare that there are no conflicts of interest regarding the publication of this manuscript.

REFERENCES

1. Guan Y, Wang S, Wang X, Sun C, Huang Y, Liu C, et al. In situ self-assembled synthesis of Ag-AgBr/Al-MCM-41 with excellent activities of adsorption-photocatalysis. Applied Catalysis B: Environmental. 2017;209:329-38.
2. Zolezzi S, Spodine E, Decinti A. synthesis, characterization, DNA binding and cleavage activity of ruthenium (ii) complexes with heterocyclic substituted thiosemicarbazones. *Polyhedron,* 2002; 21: 55-59.
3. Calvete MJF, Silva M, Pereira MM, Burrows HD. Inorganic helping organic: recent advances in catalytic heterogeneous oxidations by immobilised tetrapyrrolic macrocycles in micro and mesoporous supports. RSC Advances. 2013;3(45):22774.
4. Sun L-B, Liu X-Q, Zhou H-C. Design and fabrication of mesoporous heterogeneous basic catalysts. Chemical Society Reviews. 2015;44(15):5092-147.
5. Sazegar MR, Dadvand A, Mahmoudi A. Novel protonated Fe-containing mesoporous silica nanoparticle catalyst: excellent performance cyclohexane oxidation. RSC Advances. 2017;7(44):27506-14.
6. Li S, Qian EW, Masaaki H, Fukunaga T. Preparation of Sulfo-Group-Bearing Mesoporous-Silica-Based Solid Acid Catalyst and Its Application to Direct Saccharification. JOURNAL OF CHEMICAL ENGINEERING OF JAPAN. 2012;45(7):484-92.
7. Pal N, Bhaumik A. Mesoporous materials: versatile supports in heterogeneous catalysis for liquid phase catalytic transformations. RSC Advances. 2015;5(31):24363-91.
8. Sithambaram S, Kumar R, Son Y, Suib S. Tandem catalysis: Direct catalytic synthesis of imines from alcohols using manganese octahedral molecular sieves. Journal of Catalysis. 2008;253(2):269-77.
9. Sazegar MR, Jalil AA, Triwahyono S, Mukti RR, Aziz M, Aziz MAA, et al. Protonation of Al-grafted mesostructured silica nanoparticles (MSN): Acidity and catalytic activity for cumene conversion. Chemical Engineering Journal. 2014;240:352-61.
10. Sazegar MR, Mahmoudian S, Mahmoudi A, Triwahyono S, Jalil AA, Mukti RR, et al. Catalyzed Claisen–Schmidt reaction by protonated aluminate mesoporous silica nanomaterial focused on the (E)-chalcone synthesis as a biologically active compound. RSC Advances. 2016;6(13):11023-31.
11. Tang C-W, Wang C-B, Chien S-H. Characterization of cobalt oxides studied by FT-IR, Raman, TPR and TG-MS. Thermochimica Acta. 2008;473(1-2):68-73.
12. Robles-Dutenhefner PA, da Silva Rocha KA, Sousa EMB, Gusevskaya EV. Cobalt-catalyzed oxidation of terpenes: Co-MCM-41 as an efficient shape-selective heterogeneous catalyst for aerobic oxidation of isolongifolene under solvent-free conditions. Journal of Catalysis. 2009;265(1):72-9.
13. Fernandes DM, Silva R, Winkler Heichenletner AA. Synthesis and characterization of ZnO, CuO and a mixed Zn and Cu oxide. *Mater. Chem. Phys.*, 2009; 115: 110–115.
14. Szegedi Á, Popova M, Dimitrova A, Cherkezova-Zheleva Z, Mitov I. Effect of the pretreatment conditions on the physico-chemical and catalytic properties of cobalt- and iron-containing Ti-MCM-41 materials. Microporous and Mesoporous Materials. 2010;136(1-3):106-14.
15. Liu J, Zhang L, Yang Q, Li C. Structural control of mesoporous silicas with large nanopores in a mild buffer solution. Microporous and Mesoporous Materials. 2008;116(1-3):330-8.
16. Solovyov LA. Diffraction analysis of mesostructured mesoporous materials. Chem Soc Rev. 2013;42(9):3708-20.
17. Trong On D, Zaidi SMJ, Kaliaguine S. Stability of mesoporous aluminosilicate MCM-41 under vapor treatment, acidic and basic conditions. Microporous and Mesoporous Materials. 1998;22(1-3):211-24.
18. Triwahyono S, Abdullah Z, Jalil AA. The Effect of Sulfate Ion on the Isomerization of n-Butane to iso-Butane. Journal of Natural Gas Chemistry. 2006;15(4):247-52.
19. Alipour K, Nasirpouri F. Smart anti-corrosion self-healing zinc metal-based molybdate functionalized-mesoporous-silica (MCM-41) nanocomposite coatings. RSC Advances. 2017;7(82):51879-87.
20. Sazegar MR, Triwahyono S, Jalil AA, Mukti RR, Mohaghegh SMS, Aziz M. High activity of aluminated bifunctional mesoporous silica nanoparticles for cumene hydrocracking and measurement of molar absorption coefficient. New Journal of Chemistry. 2015;39(10):8006-16.
21. Lee AF, Bennett JA, Manayil JC, Wilson K. Heterogeneous catalysis for sustainable biodiesel production via esterification and transesterification. Chem Soc Rev. 2014;43(22):7887-916.
22. Li S-W, Yang Z, Gao R-M, Zhang G, Zhao J-s. Direct synthesis of mesoporous SRL-POM@MOF-199@MCM-41 and its highly catalytic performance for the oxidesulfurization of DBT. Applied Catalysis B: Environmental. 2018;221:574-83.
23. Dawood KM, Shaaban MR, Elamin MB, Farag AM. Catalytic activity of some oxime-based Pd(II)-complexes in Suzuki coupling of aryl and heteroaryl bromides in water. Arabian Journal of Chemistry. 2017;10(4):473-9.
24. Xavier DA, Srividhya N. Synthesis and Study of Schiff base Ligands. IOSR Journal of Applied Chemistry. 2014;7(11):06-15.
25. Maronna MM, Kruissink EC, Parton RF, Tinge JT, Soulimani F, Weckhuysen BM, et al. NbOx/SiO2 in the gas-phase Beckmann rearrangement of cyclohexanone oxime to ε-caprolactam: Influence of calcination temperature, niobia loading and silylation post-treatment. Applied Catalysis B: Environmental. 2016;185:272-80.
26. Chen B, Wang L, Dai W, Shang S, Lv Y, Gao S. Metal-Free and Solvent-Free Oxidative Coupling of Amines to Imines with Mesoporous Carbon from Macrocyclic Compounds. ACS Catalysis. 2015;5(5):2788-94.
27. Ali E, Naimi-Jamal MR, Dekamin MG. Highly efficient and rapid synthesis of imines in the presence of nano-ordered MCM-41-SO_3H heterogeneous catalyst. *Sci. Iran C, Transactions C, Chem. chemical eng,* 2013; 20: 592–597.
28. Mavrogiorgou A, Baikousi M, Costas V, Mouzourakis E, Deligiannakis Y, Karakassides MA, et al. Mn-Schiff base modified MCM-41, SBA-15 and CMK-3 NMs as single-site heterogeneous catalysts: Alkene epoxidation with H2O2 incorporation. Journal of Molecular Catalysis A: Chemical. 2016;413:40-55.
29. Rostamizadeh S, Shadjou N, Azad M, Jalali N. (α-Fe2O3)-MCM-41 as a magnetically recoverable nanocatalyst for the synthesis of pyrazolo[4,3-c]pyridines at room temperature. Catalysis Communications. 2012;26:218-24.